EUROPEAN ORGANIZATION FOR NUCLEAR RESEARCH
European Laboratory for Particle Physics

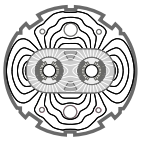

Large Hadron Collider Project **LHC Project Report 368**

Design Considerations for the LHC 200 MHz RF System

D. Boussard, E. Chiaveri, H.P. Kindermann, T. Linnecar, S. Marque, J. Tückmantel
CERN, SL Division, 1211 Geneva 23, Switzerland

Abstract

The longitudinal beam transfer from the SPS into the LHC 400 MHz buckets will not be free of losses without a lower frequency capture system and a fast longitudinal damping system in LHC. We present a complete study of a combined system using four identical copper cavities at 200 MHz delivering 3 MV total CW voltage and having still enough bandwidth to achieve fast longitudinal damping. The shape of a cavity was designed according to the accelerating mode performance, its tuning and the higher order mode spectrum with respect to the LHC beam lines and their possible attenuation. The possibility to park the cavities during coast was included. The local heat load and the corresponding cooling water distribution as well as deformations were studied and techniques to build the cavity with all ports at low cost are proposed. The parameters of the RF generators, couplers and detuning are determined. Simulations of the total LHC RF system incorporating real delays, generator bandwidth and the control loops confirm that this system is capable of capturing and damping the beam longitudinally without losses.

SL Division

Administrative Secretariat
LHC Division
CERN
CH - 1211 Geneva 23
Switzerland

Geneva, 19 January 2000

DESIGN CONSIDERATIONS FOR THE LHC 200 MHz SYSTEM

D. Boussard, E. Chiaveri, H.P. Kindermann, T. Linnecar, S. Marque and J. Tückmantel

CERN, SL Division, 1211 Geneva 23, Switzerland

1 Introduction

Detailed computer simulations of the longitudinal transfer from the SPS to the LHC (including the effect of a longitudinal damper) [i] have shown that the original transfer scheme mentioned in the Yellow Book [ii] would not work in the case of a beam emittance of 1 eVs. To cope with this situation, not unlikely considering present observations in the SPS, a 200 MHz capture RF system in the LHC has been proposed.

A satisfactory capture scenario can be achieved with 3 MV total 200 MHz RF capture voltage per beam and a maximum 200 MHz damper voltage of 100 kV [i]. As will be shown in the following these requirements can be met with reasonable safety margins using four 200 MHz cavities, providing *simultaneously* the capture and damper voltages. Contrary to the original proposal [ii], there will be no dedicated damper cavities, instead of the three initially proposed. The increase in machine impedance (four 200 MHz cavities instead of three) remains marginal.

This arrangement provides adequate damping of the injection oscillations of each newly injected batch, but cannot fight against high mode number instabilities because of the limited bandwidth of the RF power sources needed to provide the capture voltage. Although this might seem at first sight to be an unacceptable limitation, in reality it is not. Instability modes which would not be naturally damped by Landau damping cannot be suppressed by any reasonable damper system [iii].

In the following, the design choices for a combined capture-injection damping 200 MHz RF system will be presented. These are based on four cavities, designed for a maximum voltage of 1 MV each, but operationally running at 750 kV during capture.

2 The 200 MHz ACN Cavities

Although superconducting (sc.) cavities have been considered for this application (for the sake of completeness), they were rapidly rejected. The cavity shape is constrained by the beam-to-beam separation of 420 mm in the RF section and at 200 MHz a 'spherical' cavity – the proven shape for sc. cavities – does not fit in. Therefore sc. technology would have to be applied in an *unknown* domain of *geometries* and *frequency*. On the other hand the savings on the installed RF power in a situation of high beam loading are fairly modest. Therefore classical copper cavities will be employed.

2.1 Cavity shape

The cavity diameter constraint results in a quality factor and heat dissipation somewhat worse than the optimum case (e.g. the SWC 200 MHz cavities [iv] in the SPS), as shown in Table 1.

Most of the heat is produced in the long tubes ("nose cones") for which a conical shape was adopted to facilitate cooling (Fig. 1). The detailed cavity shape was obtained by imposing the condition that no important monopole mode must fall on a major beam line (every 40.08 MHz). This limits the power induced by the beam, which has to be extracted by the Higher Order Mode (HOM) couplers or dissipated in the cavity walls.

Table 1. Comparison of calculated main cavity parameters ACN vs. SWC cavities

	ACN	SWC
Frequency (MHz)	200.4	200.4
R/Q (Ω)	192	170
Q_o	30000	54000
Outer diameter (mm)	660	1000
Beam tube diameter (mm)	100	144
Dissipated power @ 1 MV (kW)	87	54
Peak electric field @ 1 MV (MV/m)	13.1	10.2

Table 2 shows a list of HOMs of the ACN cavity up to 1.5 GHz; all monopole modes are more than 0.5 MHz away from a 40.08 MHz harmonic. (The closest mode is at 1283.15 MHz.)

Table 2. All monopoles up to 1500 MHz (SUPERFISH) with R/Q and the natural (i.e. without external damping) shunt impedance R_s (upper group: symmetric modes; lower group: anti-symmetric modes)

MODE FREQUENCY (MHz)	Q	R/Q (Ω)	R_s (MΩ)
200.392	30919	192.508	5.95214
487.789	50516	17.0104	0.8593
714.617	50956	11.7906	0.6008
777.54	44095	0.34246	0.0151
944.228	78319	7.16075	0.56082
1114.502	55995	0.03439	0.00193
1252.633	69028	0.2107	0.01454
1285.083	75345	1.96093	0.14775
1382.505	63256	0.28963	0.01832
1486.723	70435	0.10265	0.00723
247.294	29213	3.9236	0.11462
633.172	44002	2.68364	0.11809
748.164	45515	8.31742	0.37857
934.636	48972	0.09705	0.00475
1109.467	66193	9.70991	0.64273
1283.151	56155	0.64556	0.03625
1328.024	69381	1.13926	0.07904
1445.858	57121	0.73813	0.04216
1499.03	73731	4.46952	0.32954

As shown in Fig. 1 the "corners" of the cavity cross-section have been rounded to facilitate cleaning and to minimise multipacting (to some extent).

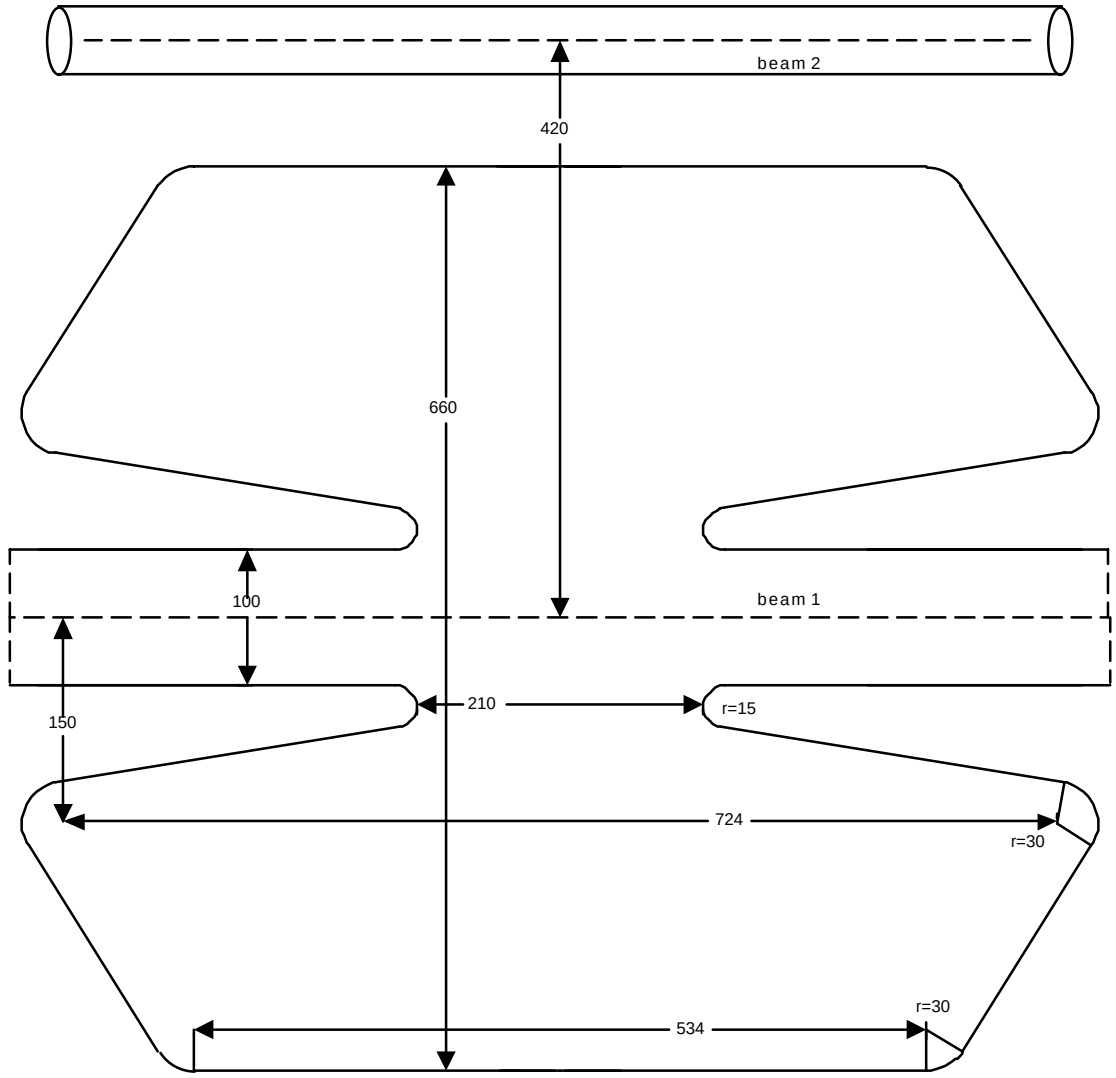

Fig. 1. 200 MHz ACN cavity geometry

2.2 Cavity cooling

The theoretical cavity dissipation for 1 MV accelerating voltage is 87 kW at 20ºC. Assuming an average temperature increase of the copper of less than 20ºC, the maximum power to be evacuated from the cavity is about 100 kW. Fifty percent of it is produced on the two inside nose cones, 30% on the two outside large cones and 20% on the outer cylinder.

Cooling is achieved with demineralized water (input temperature 20°C, pressure 6 bars). The total flow, for a temperature increase of the water limited to 20°C amounts to 1 ℓ/s (3.6 m^3/h), which must be split as follows:

- 0.9 m^3/h for each nose cone
- 0.54 m^3/h for each large outside cone
- 0.72 m^3/h for the cylinder

Each nose cone has four helical channels (cross-section 8 x 5 mm^2), two on the outside and two on the inside. They are spaced 4 mm apart, providing a total water-to-copper surface of 0.65 m^2. The water speed must be 1.6 m/s, leading to a turbulent flow (Reynolds number

10900) and a heat transfer coefficient, from water to the copper cavity surface, of 6000 W/m^2/K. The average copper-water temperature drop will be 5.4 K.

Each large outside cone will be fitted with two spiralled cooling channels (cross-section 8×5 mm^2). They are spaced 4 mm apart, providing a total water-to-copper surface of 0.37 m^2. The water speed must be 2.5 m/s, leading to a turbulent flow (Reynolds number 17000) and a heat transfer coefficient, from water to the copper cavity surface, of 6100 W/m^2/K.

The outer cylinder is cooled by two helical cooling channels (cross-section 8×5 mm^2, four turns on each side) and by two cooling jackets. The helical cooling channels provide a water to copper surface of 0.45 m^2. The water speed must be 1.9 m/s for 0.40 m^3/h water flow (Reynolds number 13000) leading to a heat transfer coefficient of 6200 W/m^2/K.

Two cooling jackets (one cooling channel per jacket, section 15 x 5 mm^{2,} length 5 m) provide a water to copper surface of 0.4 m^2. The water speed must be 1.15 m/s, for 0.36 m^3/h water flow (Reynolds number 9600), leading to a heat transfer coefficient of 4300 W/m^2/K.

The complete cavity can be modelled with the finite element simulation program ANSYS, using the input power flow distribution given by SUPERFISH and simulating cooling with an average heat transfer coefficient of 4000 W/m^2/K (pessimistic value). Fig. 2a shows the temperature map and Fig. 2b and 2c show the radial and longitudinal distortions of the cavity under temperature.

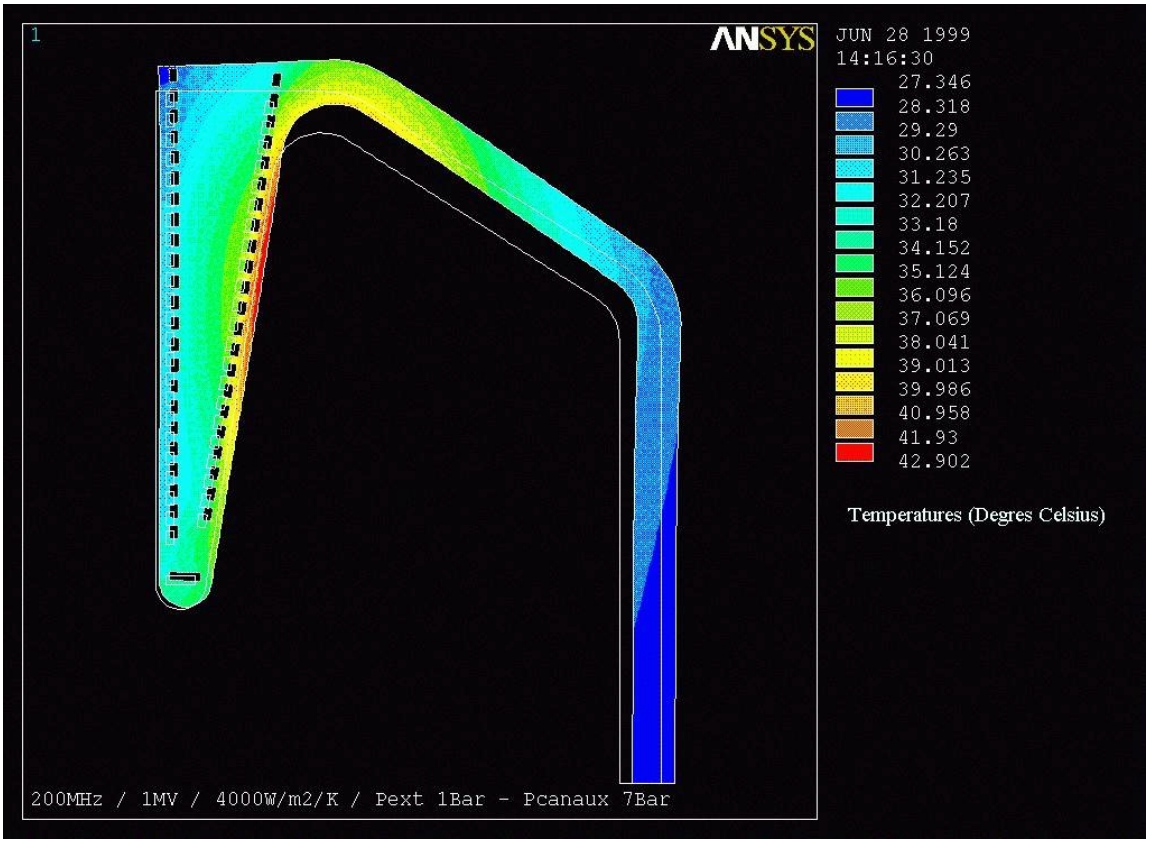

Fig. 2a. Temperature map of ACN

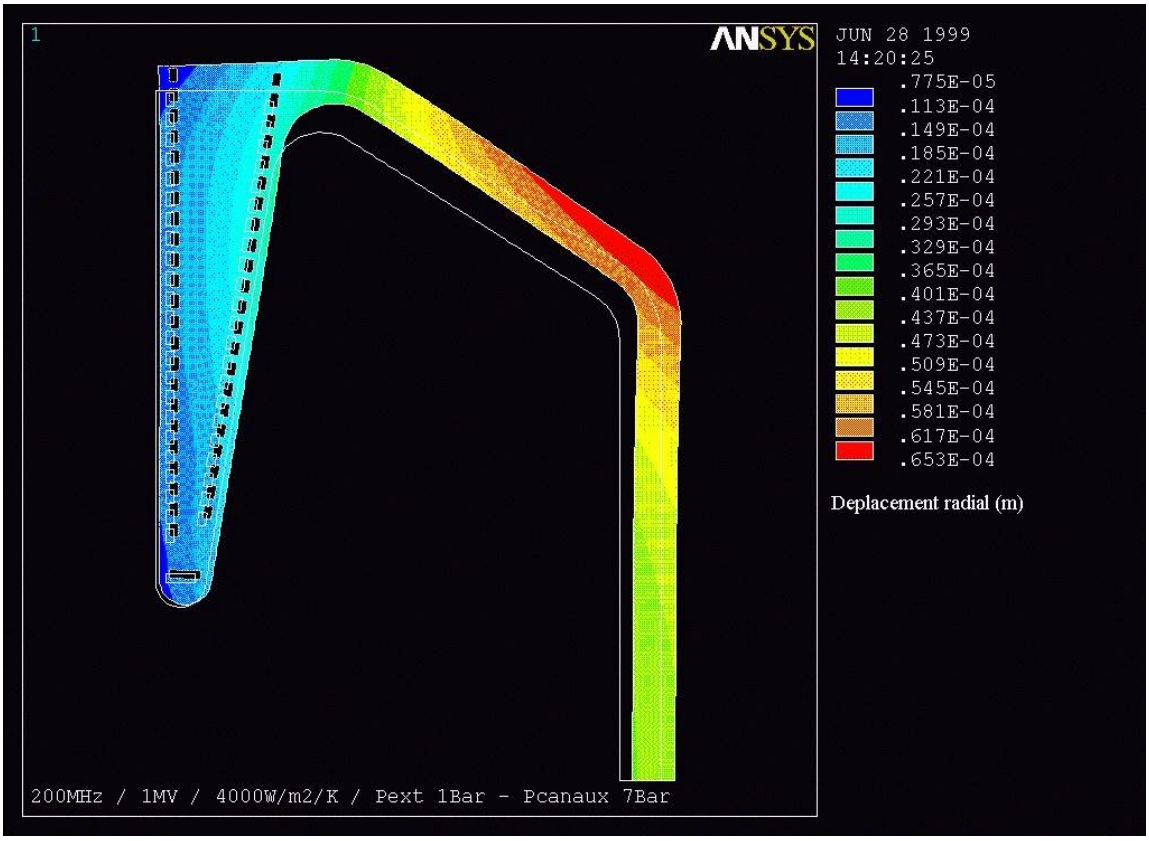

Fig. 2b. Radial distortions

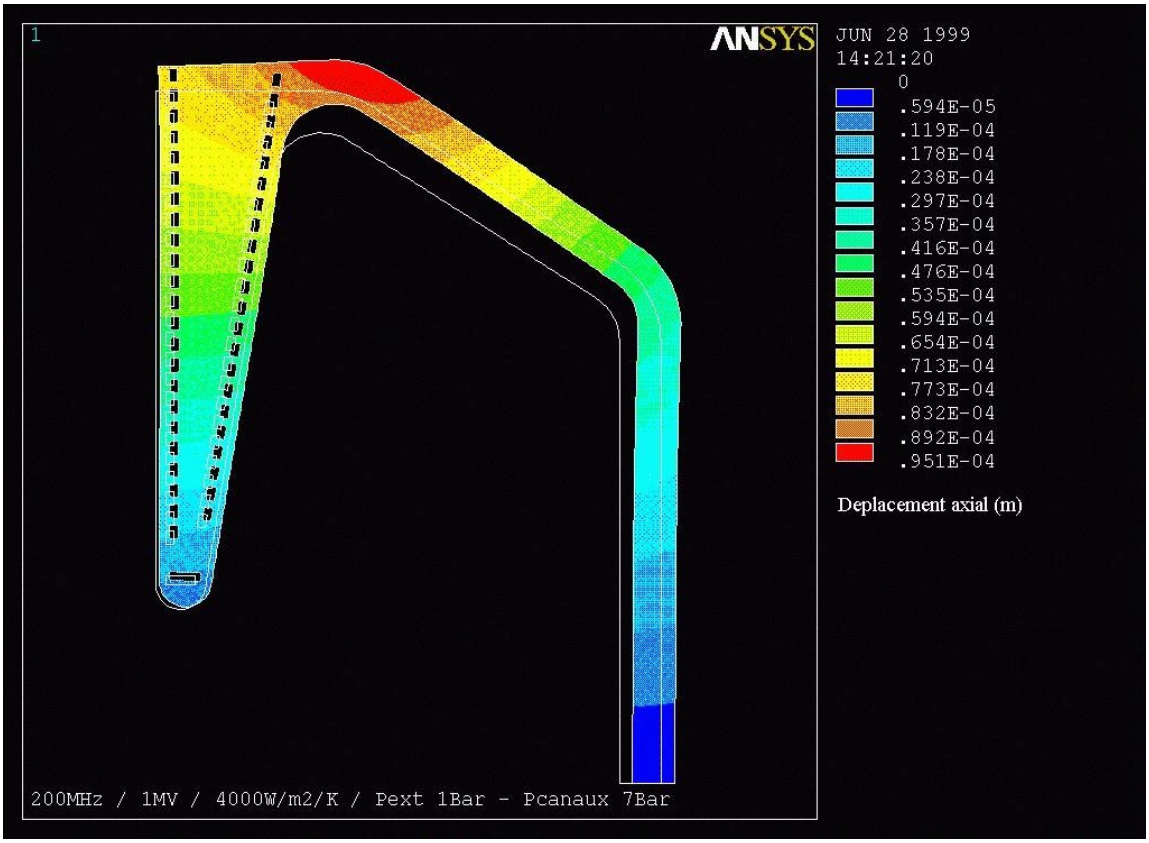

Fig. 2c. Longitudinal distortions

The temperature reaches a maximum of 43°C on the slope of the nose cone and the maximum internal stress amounts to 23 MPa, i.e. <10% of the elastic limit of the copper.

The program also calculates the change of resonant frequency of the cavity and gives:

$$\Delta f = -45 \text{ kHz @ } 1 \text{ MV}.$$

2.3 Higher order mode couplers

The most prominent higher-order modes (HOM) of the ACN cavity (monopoles and dipoles) are listed in Fig. 3a and 3b, together with their magnetic field distribution on the cavity wall. As it would be very advantageous to re-use the HOM couplers from the SWC cavities (predominantly magnetically coupled), we can try to estimate the achievable damping on the ACN cavities using those. To be able to couple with practically all modes shown in, we propose to install two magnetic HOM couplers located at ± 120 mm from the cavity (longitudinal) mid-plane. This corresponds to about point 15 on the abscissa of Fig. 3a and 3b. At this point all modes considered (except the dipole at 457 MHz) have a magnetic field larger than 10^3A/m/$^{\text{Joule}1/2}$ stored energy.

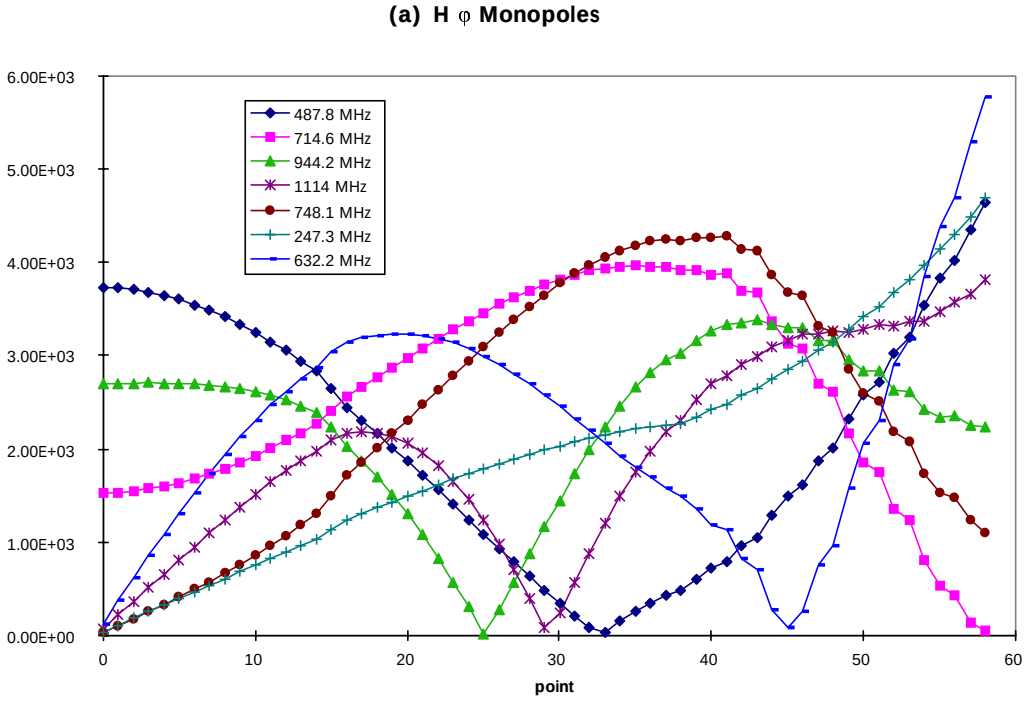

Fig. 3a. Surface field distribution H_φ of monopole modes.
The horizontal axis expresses the mesh point along the cavity surface, point 0 at the cavity mid-plane, point 58 at the lower end of the large outside cone.

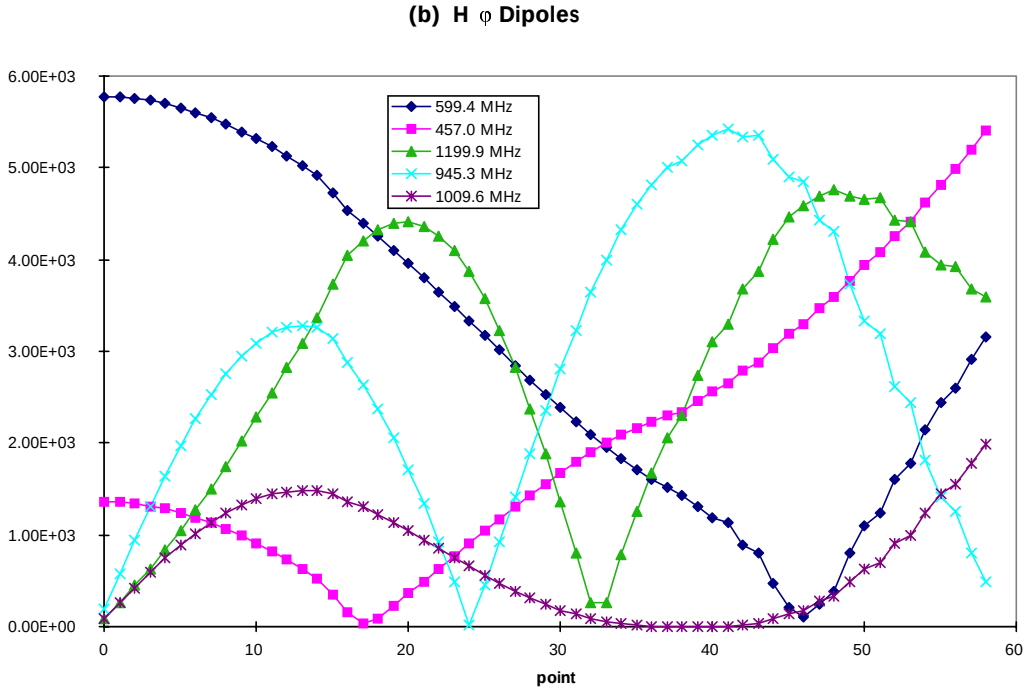

Fig. 3b. Surface field distribution H_φ of dipole modes.
(horizontal axis as in Fig. 3a)

We estimate the performance of the SWC loop placed in the ACN cavity using the relation

$$Q_H = \frac{k\ U_{st}}{f\ H^2}$$

where k is a parameter which depends on the loop effective area (the loop is assumed to be compensated), f the frequency of the HOM, U_{st} the cavity stored energy and H the magnetic field of the mode at the loop location. In order to estimate the parameter k we choose the 447 MHz mode in the SWC cavity having a non-vanishing magnetic field at the mid-plane, which is most similar to the first mode in the ACN cavity. Its magnetic field is 2.6×10^3 A/m/Joule$^{1/2}$ and its measured damped Q is 2800 (1400 for two loops) [iv].

For the ACN cavity we find, for three typical modes (longitudinal) at 487, 247 and 714 MHz, the results shown in Table 3. The total cavity Q is obtained with four couplers installed (two pairs at 90° to couple also to the two polarisations of the dipole modes).

Table 3. Parameters of the most prominent monopole HOMs.

f MHz	**R/Q Ω**	**H_φ (kA/m/ Joule$^{1/2}$)**	**Q/coupler**	**Total Q**	**R (four cavities) kΩ**	**Instability growth rate $\Delta\omega_s/\omega_s$** (nominal intensity)
247	3.9	1.2	23787	5946	93	9×10^{-4}
487	17	2.2	3590	897	61	8×10^{-4}
714	11.8	2.8	1511	377	18	2.5×10^{-4}

These results show that there is a fair chance of damping properly the ACN cavity HOMs by re-using the SWC couplers. The most critical cases (247 MHz monopole, 457 MHz dipole) will probably be damped more than calculated, because of the electric coupling of the HOM couplers. This has not been considered here but has been shown to exist in the SWC cavities where modes having no magnetic field on the SWC mid-plane are nonetheless substantially damped [iv]. In any case the HOM locations seem to be adequate to satisfy the LHC requirements with magnetic, electric or combined HOM couplers.

Note that, at the beginning, we considered placing magnetic HOM couplers at the mid-plane and on the end cones, where some of the HOMs have their highest field. This solution was, however, rejected because of the excessive 200 MHz RF current density in the RF spring contacts of the HOM couplers (> 40 A/cm, as compared to 25 A/cm in the SWC case).

The longitudinal mode at 1283.15 MHz, closest to a beam line, may fall exactly on the 32^{nd} harmonic of the beam frequency (due to cavity tuning or to the influence of the ancillary equipment). The maximum power that can be extracted by the HOM couplers corresponds to the case where Q_{ext} (couplers) = Q_o = 56000. For the nominal 0.56 A beam, the total power lost in this mode is about 1 kW, split equally between the cavity walls and the four HOM couplers (125 W/coupler, easily extracted).

Instability growth rates can be evaluated for the nominal beam from the results of Table 2, where R_s is the total shunt resistance, corresponding to four cavities and $\Delta\omega_S$ the resulting instability growth rate. ($\omega_S/2\pi$ is the synchrotron frequency) The worst case is during storage when the bunches are shortest (total bunch length 30 cm). In all cases there is a reasonable safety margin with the Landau damping limit $\Delta\omega_S/\omega_S = 0.025$ [iii].

2.4 Cavity tuner

- The cavity tuner must have enough range to cope with the following requirements:
- Correction of the frequency drift with temperature, estimated to be –45 kHz from 0 to 1 MV accelerating voltage
- Compensation of reactive beam loading in the "half-detuning" mode (see 3.1). At full beam (0.56 A d.c.) and 750 kV/cavity, the cavity frequency must be lowered by 16.5 kHz.
- Parking the cavities when not in use. Although passive damping looks more attractive, it would be interesting to keep the possibility of parking the cavities symmetrically with respect to the RF line (two pairs). A detuning of the cavities of ± 100 kHz seems adequate to keep the beam voltage low enough in each cavity.
- Correction of the static errors. The thickness of the final weld determines the exact cavity length; it is known with an uncertainty of about 0.1 mm, which corresponds to a frequency uncertainty of about 35 kHz.
- Correction of the frequency drift during pumping down of the cavity. The mechanical deformation is expected to be negligible, but the change due to the ε_r of air is about 60 kHz.

The effect of the auxiliaries (HOM couplers, RF coupler, ports etc.) can be estimated from the SWC experience [iv] and leads to a fairly large uncertainty (several hundred kHz) on the exact cavity frequency. It is not considered necessary to correct those with the movable tuner, but to adjust the exact length of the gap, by measuring the resonant frequency with all auxiliaries in place, before the final welding.

It is proposed that the SWC piston tuners (∅ 146 mm, stroke 100 mm, no sliding contacts) located at the cavity mid-plane should be re-used. Positioning the tuner in the mid-

plane minimises the possible excitation of a TEM mode in the coaxial line formed by the piston and the cavity port wall and therefore the possible heating of the tuner bellows.

The magnetic field at the cavity is 2170 A/m for the ACN cavity (@ 1 MV) compared to 2500 A/m for the SWC cavity, at its maximum voltage (1 MV). The tuner heating and the tuner range should therefore be smaller, in the ACN cavity, by the factor $(2170/2500)^2 = 0.75$, neglecting the influence of the electric field (vanishing on the mid-plane). This ensures correct functioning of the SWC tuner in the ACN cavity (no overheating) and gives a tuning range of 400 kHz × 0.75 = 300 kHz for a 100 mm stroke, which should be adequate.

The tuner speed is not a critical parameter; in the "half-detuning" mode the tuner position is the same with and without beam. In the case of an imperfect setting of the tuner, for a given operating condition, the necessary RF power will increase. Consequently the speed of the tuner will determine the duration of the excess RF power demand, which must be compatible with the RF power source capability. Typical response times of the SWC tuners are in the 50 ms range, very similar to other types of tuner (e.g. magnetostrictive tuner in superconducting cavities). They are not meant to respond to synchrotron frequency oscillations (60 Hz at injection).

2.5 Fundamental mode couplers

The external Q of the main RF coupler is defined in such a way as to minimise the power required to operate the cavity in the "half-detuning" mode (see 3.1) at maximum beam current (0.56 A/beam). Assuming an operating voltage of 750 kV/cavity, the optimum values are the following:

$Q_{ext} = 6100$ Forward Power: 145 kW (CW)

for a stabilised beam (zero stable phase). During injection oscillations, the peak power is higher (250 kW for a 20° phase error).

The coupling to the cavity can be achieved with a magnetically coupled loop in the cavity mid-plane. The loop, assumed to be compensated, would have an area of about 20 cm^2, if connected to a 50 Ω line. The ACN coupler could be a scaled-down version of the new SPS travelling-wave cavity coupler, now under design. The loop is connected to a λ/4 shorted stub line (50 Ω), to provide compensation of the loop inductance and to bring cooling water in the loop conductor. The stub line is aligned with the coupler axis (perpendicular to the cavity wall surface) and connected to the RF line with an elbow, all these elements being under vacuum. The coaxial window is on the RF line ($6^1/_4$" diameter, for a peak forward power of about 300 kW), which runs parallel to the cavity axis.

The ACN cavities will also be equipped with movable dampers to provide passive damping where the cavities are not in use, especially during coast. It is proposed that *two* SWC dampers (stroke 100 mm, loop dimensions 120 × 60 mm^2) will be used per ACN cavity. They would be placed symmetrically at ± 120 mm from the cavity longitudinal mid-plane, where the magnetic field is practically the same as at the mid-plane of the SWC cavity (1700 A/m/$Joule^{1/2}$ stored energy). Consequently the achievable damped Q is about half that of the damped SWC cavities, i.e. 80/2 = 40.

The total power dissipated in the two damping loops would be about 5 kW, i.e. 2.5 kW in each of the SWC 5 kW loads. This safety margin looks adequate, even considering the uncertainty of the evaluation, which cannot take into account the magnetic field distortions due to the HOM couplers, located close to the damping loops (Fig. 4).

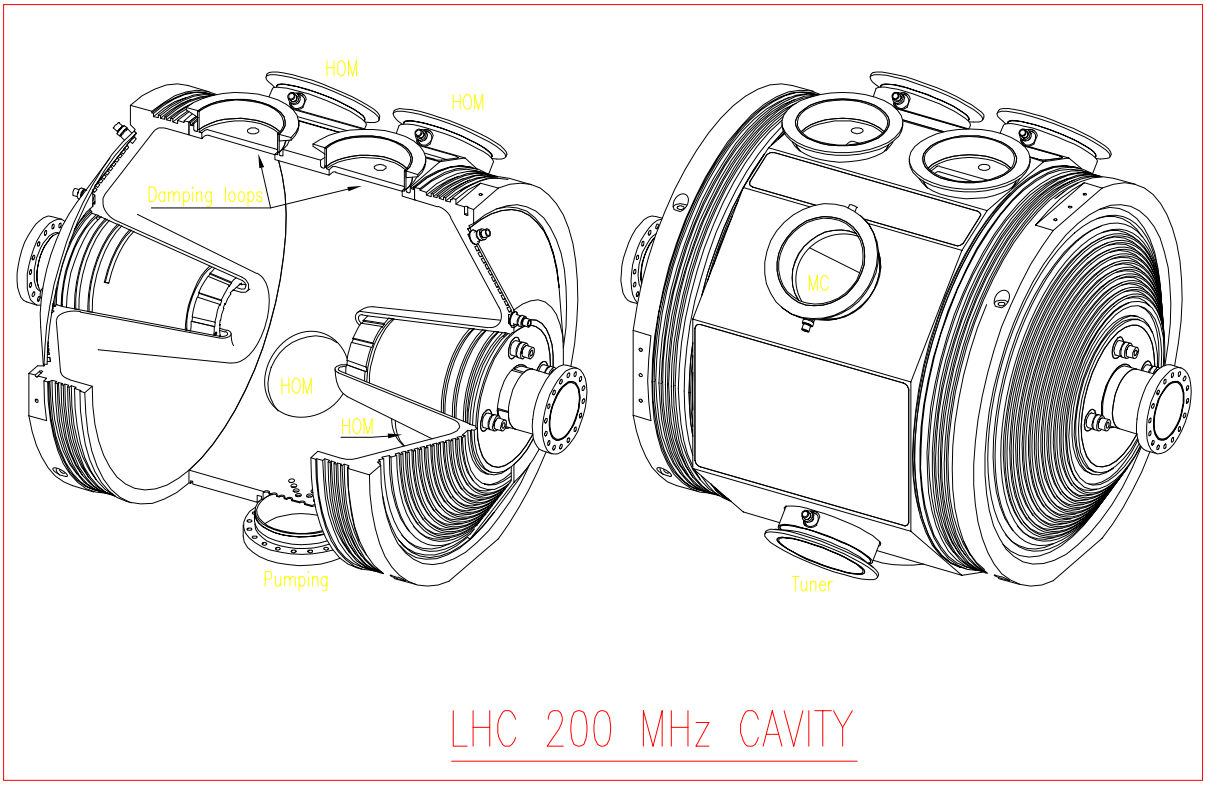

Fig. 4. Cavity construction

The residual impedance (30 kΩ for the four ACN cavities) is low enough to guarantee beam stability with natural Landau damping (with a large safety margin) when the cavities are not in use.

During the transient phase of the movable dampers (~ 1 s duration) the cavities must be actively damped (full beam compensation, see 3.3) by the power amplifier. As with the tuner, the speed of the mechanical movement of the damper determines the duration of the excess RF power demand.

The initial difficulties experienced with the SWC bellows, during the first years of operation, are of no concern for the ACN cavities where the frequency of the bellows movements is expected to be about one per day as compared to one every 14 s for the SWC.

2.6 Cavity construction (Fig. 4)

The mechanical design of the ACN cavity is based on three solid copper OFHC forgings, machined and electron-beam (EB) welded. The two end parts are identical; they are machined to produce the hollow nose cones, the cooling spirals on the outer cylinder and the end cones. There will be no join or weld in the high current density area, or between cooling water and vacuum. The central cylinder (octagonal on the outside), forged and machined, contains all cavity ports: one tuner, one main coupler, four HOM dampers, two fundamental-mode dampers and one vacuum pump. For each port, the stainless steel flanges are brazed onto a copper cylinder, which is subsequently EB welded on the cavity cylindrical part. As it is foreseen that some SWC ancillary equipment will be re-used, the standard SPS flanges will be used, where necessary. The diameter of all ports is the same (∅ = 150 mm); it should be sufficient to permit EB welding from the inside, if necessary.

The nose cone cooling is achieved with a copper cone, with machined spiral grooves, which is inserted into the hollow nose cone and EB-welded. Each cavity end is cooled by machined grooves, which are subsequently covered with a thin copper sheet EB-welded onto it. They also have cooling spirals machined on their cylindrical part, which are also covered by an EB-welded thin cylinder.

The central cylinder will be cooled by flat machined cooling jackets welded on the free outer surfaces of the octagon and by cylindrical cooling jackets on most of the cavity ports.

Of the two main cavity welds, which join the two end parts to the central cylinder, one can be done from inside, resulting in a weld with good surface quality. The last one, which must be undertaken only after a precise determination of the cavity frequency, with all ancillary equipment in place, is very likely to be done from the outside, and needs special precautions to guarantee also a good surface quality.

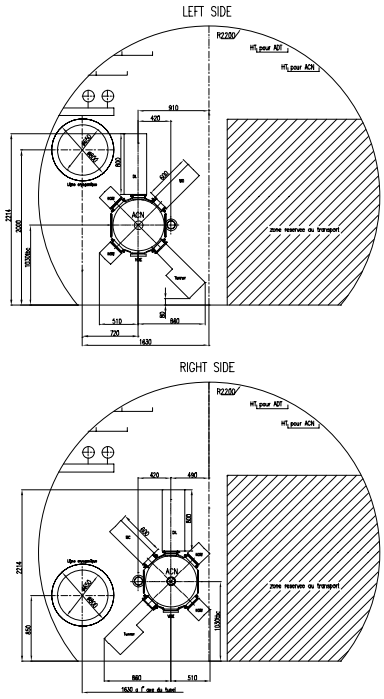

Fig. 5. Transverse layout of ACN cavities

Fig. 5 shows the transverse layout of the ACN cavities in the LHC tunnel. As with the ACS cavities, the main cryogenic transfer-line must be shifted vertically to accommodate the transverse dimensions of the cavity and its ancillary equipment.

3 Modes of Operation and Power Requirements

3.1 "Half detuning" operation

Each ACN cavity and its RF power amplifier will be part of an RF feedback loop, whose purpose is to keep the RF voltage constant (in amplitude and phase) irrespective of the beam current. This ensures ideally the same behaviour for all bunches of an injected batch. We assume in the following a perfect RF feedback (with infinite gain) which keeps the RF voltage vector $\overrightarrow{V_{RF}}$ constant. The RF feedback will probably be a combination of direct feedback (gain limited by the overall loop delay) and one turn delay feedback, to achieve the

highest gain and speed. The effect of a limited feedback gain is evaluated by simulations in chapter 3.5.

In Fig. 6, the RF component of the beam current is represented by a vector $\vec{I}_b$, in quadrature with $\vec{V}_{RF}$ (as $\varphi_s = 0$ on the injection plateau). The total current $\vec{I}_t$ in the cavity is the vector sum of $\vec{I}_b$ and the generator current $\vec{I}_g$. In the classical case of a continuous beam $\vec{I}_g$ and $\vec{V}_{RF}$ are kept in phase by the servo-tuner which compensates the reactive part of beam loading ($\vec{I}_g = \vec{I}_{go}$ in Fig 6a). If there is a gap in the beam train (longer in duration than the response time of the RF feedback but much shorter than the response time of the tuner) and if we assume the tuner position remains unchanged, the RF voltage vector $\vec{V}_{RF}$ (still constant) will be produced during the gap, when $\vec{I}_b = 0$, by a new generator current $\vec{I}_g = \vec{I}_t$. The power demand, during the gap, will be higher than during the batch by the factor $\left(|i_t| / |i_{go}|\right)^2$.

To avoid a higher power demand to the generator, we make the two generator currents equal in amplitude during the beam batch and during the beam gap. This corresponds to the case of Fig. 6b where the detuning of the cavity is half the value relative to a continuous beam of the same batch intensity.

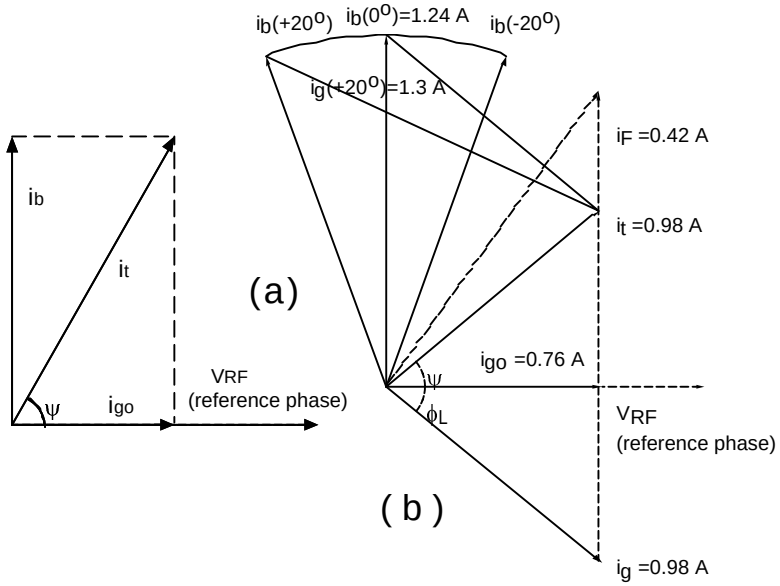

Fig. 6. Vector diagram of RF currents in cavity (reference phase is $\vec{V}_{RF}$)

Once the cavity detuning is defined, we optimise the cavity coupling to achieve overall minimum power. In the case of a matched generator (with circulator) the optimum coupling (its Q_{ext}) is given by ref. [v]:

$$Q_{ext\ opt} = R_g / (R/Q)$$

$$\frac{1}{R_g^2} = \left(\frac{i_b}{2V_{RF}}\right)^2 + \frac{1}{R'^2}$$

$R' = \frac{R}{Q} \times Q_o$ being the cavity shunt resistance.

In this case the minimum power needed to operate the cavity is given by:

$$P_{opt} = \frac{V^2}{4R_g} + \frac{V^2}{4R'}$$

For the LHC parameters at injection (V_{RF} = 750 kV per cavity, i_b = 1.24 A @ 200 MHz, R/Q = 192 Ω, R′ = 5.7 MΩ) we obtain:

R_g = 1.18 MΩ, $Q_{ext\ opt}$ = 6100, P_{opt} = 145 kW

These figures correspond to the equilibrium situation, after the longitudinal oscillations at injection are completely damped. To take into account the fact that the bunches from the SPS may be injected with phase errors, the vector diagram of Fig. 6b will be slightly modified. The new $\vec{i_b}$ vector, instead of being in exact quadrature with $\vec{V_{RF}}$ is now rotated in phase by the injection phase error (typically up to ± 20° @ 200 MHz). Depending on the sign of the phase error, this new situation will require either more or less generator power to maintain $\vec{V_{RF}}$ constant, with the same detuning angle. The peak power demand, proportional to the square of the modulus of the vector $\left(\vec{i_{b\,(+20°)}} - \vec{i_t}\right)$, can be directly estimated in Fig. 6b. It gives $|i_g|$ = 1.3 A and $\hat{P}$ = 250 kW.

The generator power will be modulated at the synchrotron frequency (P_{max} = 250 kW) while the injection oscillations are being damped. Then the power will stay constant (P = 145 kW) until a new batch is injected.

For the sake of completeness, the corresponding figures in the case of 1 MV/cavity (one cavity out of service, or capture voltage at 4 MV) are given below:

R_g = 1.55 MΩ $\quad Q_{ext}$ = 8000 $\quad P_{opt}$ = 200 kW $\quad \hat{P}$ = 360 kW

Note that the peak powers obtained here could be reduced by optimising the coupling for the case of a +20° phase error. This would, however, result in a higher CW power and was therefore not considered here.

3.2 Damping of injection errors

In the simulations of ref. [i], a feedback voltage of 100 kV maximum is sufficient to damp properly an injection oscillation of ± 20° (@ 200 MHz) initial amplitude. The latter may results from an uncertainty on the LHC dipole magnetic field, from synchronisation and signal transmission errors, or from a phase modulation on the SPS beam due to the high impedance of the travelling-wave structures. The first two sources lead to a constant phase error along the newly injected batches, and a global oscillation of those, which can be damped by the ACN cavities, as explained below.

The maximum 100 kV correction voltage (shared by the four cavities) is applied when the beam is in quadrature with $\vec{V_{RF}}$ (zero phase error, maximum energy error) as an additional 25 kV voltage, in quadrature with the unperturbed $\vec{V_{RF}}$. The vector diagram of Fig. 6b becomes slightly modified (25 kV added in quadrature to 750 kV) and the change of generator current required remains negligible. This corresponds to the new equilibrium situation, along the injected batches.

However, contrary to the previous case of chapter 3.1, where the RF voltage remained constant, a change of cavity voltage from its initial equilibrium value (before injection) to its

new value, with feedback voltage added, must be obtained during the beam gap. This requires an additional RF current $\vec{i}_F$ given by the equation:

$$\frac{dV}{dt} = \frac{1}{2}\frac{R}{Q}\omega_o\, i_F$$

Taking the worst case dV/dt = 25 kV in 0.5 μs (useful length of a 1 μs gap), an additional RF current i_F = 0.42 A, in quadrature with the unperturbed $\vec{V}_{RF}$ must be applied to the cavity, during the beam gap (i.e. when $\vec{i}_g = \vec{i}_t$). From Fig. 6b we obtain $|\vec{i}_F + \vec{i}_t|$ = 1.3 A, which corresponds to a peak power of 250 kW, with the selected cavity coupling.

The low-level circuitry of the beam damping system must be designed in such a way as to provide the proper command to the RF power amplifier during the beam gap, to reach and maintain the required voltage along the newly injected batches.

3.3 Full beam compensation

We have seen in the previous chapter that a peak power of 250 kW must be made available to cope with injection errors and injection damping. This power corresponds to 1.3 A generator current, slightly above the RF component of the beam current (1.24 A at injection). This opens up the possibility of full beam compensation when the cavity voltage is brought to a low value, for instance at the end of the injection plateau. In this situation, the cavity can be kept under control, with RF feedback, for a vanishing RF voltage and irrespective of the tuner position (contrary to the "half detuning" operation). Here the RF generator delivers exactly the opposite of the beam current to the cavity. At this moment it is possible to introduce the passive dampers in the ACN cavity and strongly reduce its impedance, without affecting the amplifier operation. Then the amplifier can be safely switched off without perturbing the beam (very little voltage on the cavity before and after switch-off).

All this operation should be done, hopefully, fast to keep the amplifier high power operation as short as possible. A typical figure is about 1 s.

3.4 RF power amplifiers

The cavity must be connected to its power amplifier via a circulator, which directs the reflected wave to a terminating load. This configuration not only leads to the minimum RF installed power for a given cavity voltage and beam current, but also opens up the possibility of combining easily (in a 50Ω matched system) several RF power amplifiers.

The most appropriate solution here seems to combine four SWC amplifiers (60 kW CW, up to 90 kW for 1 s) via two stages of combiners (three hybrids per cavity). This arrangement gives ample safety margin (240 kW CW, 360 kW peak) and even permits operation with only three cavities active.

The amplifiers, combiners, circulator and loads can be installed in the klystron gallery. Care must be taken to keep the overall RF loop delay at its minimum value. This may imply in particular some modifications to the existing driver amplifier.

The four existing HV power supplies (10 kV, 1.1 MVA each) feeding the SWC amplifiers will be re-used for the ACN amplifiers. Each power supply will feed the amplifiers and drivers of two ACN cavities.

3.5 Simulations

The LHC RF system has two sub-systems at 200 and 400 MHz operated under various conditions during the different phases of an LHC fill. Due to the large beam current both sub-systems strongly interact with the beam and are thus coupled together. A simulation program

has been written to evaluate in detail the behaviour of the LHC RF system and to complement the simple analysis presented above. It simulates non-ideal cases, e.g. non-infinite gain of the feedback loops, a beam with gaps, non-uniform batch density, cavities working as longitudinal damper etc. The program has evolved in such a way that it already offers the possibility of running 'machine development studies' to examine many parameters and to find the best settings and the limits of the system. This program will certainly remain useful once LHC starts operation obtaining offline a better interpretation of the observations.

The essential program features are as follows:

- The RF system is treated as several (up to six) independent subsystems. Each subsystem represents a number of *identical* units with a cavity, its generator and their loops; for LHC there must be (at least) two subsystems: the eight superconducting 400 MHz cavities and the four 200 MHz copper cavities. Each cavity can be equipped with a classical RF feedback, which takes into account cable delay and amplifier bandwidth. Saturation of the RF amplifiers is also taken into account.
- A one-turn-delay RF feedback can also be introduced on each cavity.
- Each cavity can additionally be driven by a signal obtained from beam data processed to make the cavity work as a longitudinal damper.
- All cavity, generator and loop parameters can be varied according to the RF manipulations envisaged.
- A generator trip can be simulated on one (or more) cavities by setting up the tripping cavities as an additional separate subsystem: e.g. the eight superconducting cavities can be set up in the simulation as one subsystem with seven and one with a single cavity. The latter subsystem can trip while all other cavities continue to work independently.
- Bunches are considered as point charges. The bunch length is taken into account as a form factor depending on the RF frequency in the corresponding subsystem. Bunches can be injected with any error in phase or energy.
- Each bucket may or may not be occupied to simulate any LHC beam pattern, in particular during the injection process.
- The charges of individual bunches along the ring may also be set individually to simulate batches received from the SPS with non-uniform distribution. Slow beam losses (during coast) or sudden beam dump are also possible.
- The program calculates the evolution of the various RF and beam parameters: voltages, powers, phase and energy errors etc.

Data used in the simulations correspond to the nominal parameters of the two RF subsystems in their various operating conditions as shown in Table 4.

Table 4. Nominal parameters for the two RF systems in LHC for various operating conditions

	200 MHz Cu injection	200 MHz Cu parked	400 MHz s.c. injection	400 MHz s.c. bunch transfer	400 MHz s.c. coast
Number cav.	4	2+2	8	8	8
f [MHz]	200.4	200.4	400.8	400.8	400.8
R/Q [c.Ohm]	192.5	192.5	45	45	45
Q_o	31000	31000	2.00E+09	2.00E+09	2.00E+09
Q_{ext}	5000	<100 (passive damping)	40000	40000	160000
Pmax [kW]	300	generator off	300	300	150 (reduced)
BW [MHz]	2	-	1	1	1
delay [ns]	500	-	500	500	500
V [MV]	0.75	(0)	(0)	1	2
f [kHz]	-16	(±100)	(-4.5)	-4.5	• -3.5

The program passed tests for different mathematically calculable conditions with smooth beam. The RF feedback – without beam - becomes unstable at a *critical* gain exactly predicted by theory. Furthermore the simulated beam develops longitudinal coupled bunch (dipole) oscillations caused by cavities switched off and detuned ('parked') with growth rates corresponding well to estimates for a smooth beam with equivalent current.

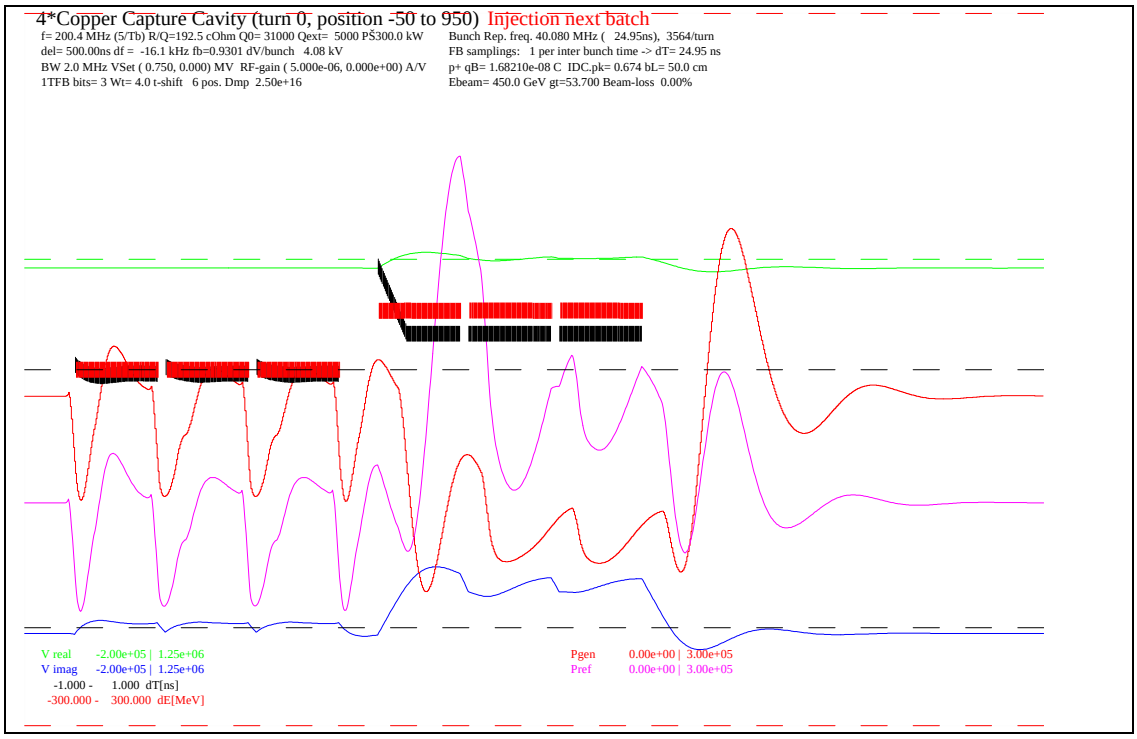

Fig 7a. Injection of second SPS batch (3 PS batches)

With the parameters of table 4 the critical gain g_{crit} of the RF feedback of the 200 MHz subsystem is 16. The characteristic ringing time $T_{ring} \approx T_{delay} / \ln(g_{crit}/g)$ becomes 0.35 μs if we take $g = g_{crit}/2 = 8$ to stay away from the instability limit. Unfortunately T_{ring} is not very

small compared to the time between SPS batches (about 1 μs) and transient effects are therefore important.

Due to the low gain in the 200 MHz RF feedback the residual voltage swing between 'beam on' and 'beam off' is still ±75 kV in quadrature with V_{RF}, i.e. in phase with the beam. It is therefore necessary to add the one-turn feedback (with a gain four times that of the RF feedback and a filter parameter k = 7/8). The voltage swing is then reduced to ±15 kV.

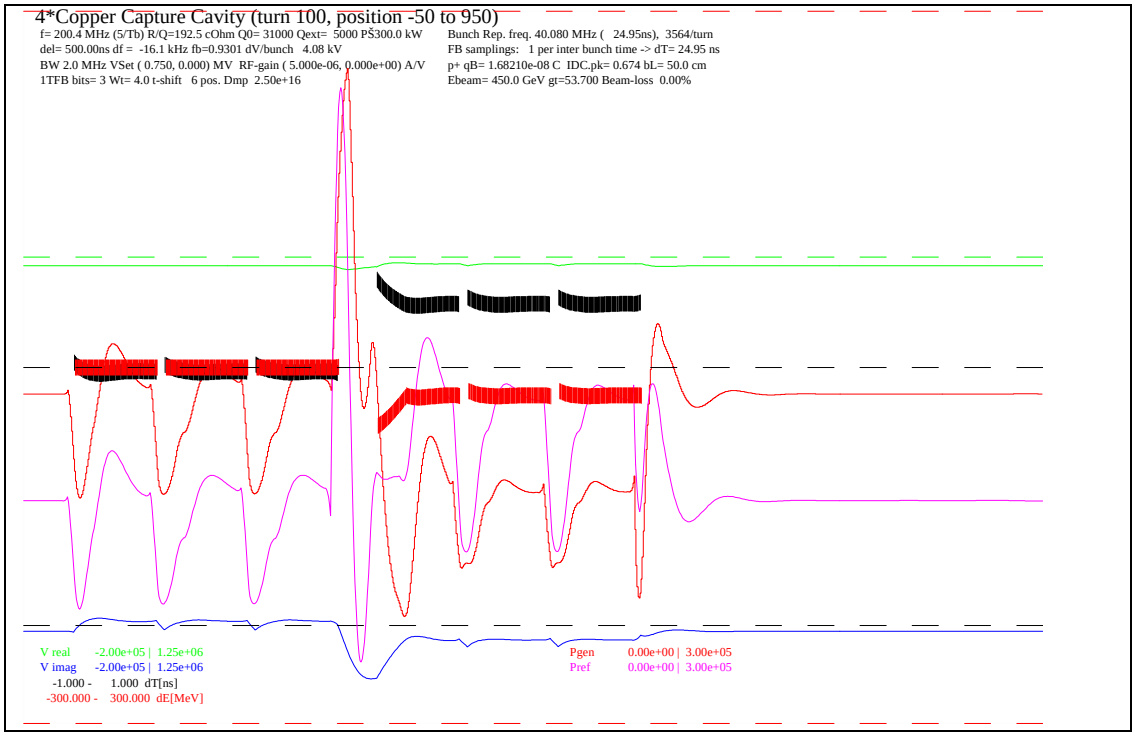

Fig 7b. After 100 turns with one turn delay feedback and longitudinal damping (damper gain 2.5 10^{16} V/(s/turn))

The possibility of operating all four 200 MHz cavities simultaneously as capture cavities and longitudinal damper system was examined. Simulations showed that this was not possible if the cavities were operated with RF feedback only. In this case the transients were comparable in magnitude to the damper voltage and it turned out that beam oscillations were amplified instead of being attenuated. However, adding the one-turn-delay feedback reduced the transients sufficiently to obtain fast enough damping (faster than 1000 turns where filamentation starts to become important [1]).

This operation is shown in Fig. 7a to 7c. The 200 MHz accelerating voltage is drawn in green (set value dashed), and its quadrature component – in phase with the nominal beam – in blue (range -0.2 to +1.25 MV), the generator power in red and the reflected power in magenta (range 0 to 300 kW). The (average) particle energy in the bunches is represented by the red bars (ΔE-range ±300 MeV), the relative time position of the bunch charge centre by the black bars (Δt-range ±1 ns). The horizontal time axis covers about 25 μs (28% of a machine turn) and starts 1.25 μs before the first bunch arrives[1]. Since no more batches come in this turn and transients die out at the right side of the plot, all parameters remain stable – right and left side of the plot match – and this part of the turn is not shown.

[1] The range corresponds in fact to 1000 inter-bunch times T_b=1/(40.08 MHz) from position –50 to +950, the first bunch of the first batch defines position 0. The whole ring has 3564 available positions.

In Fig. 7a the RF parameters and the beam are presented at injection of the second SPS batch. The first SPS batch (three PS batches) is already attenuated: the beam energy is uniform at the nominal energy, i.e. the red bars are centred. The second SPS batch was just injected with worst case errors in energy and phase ($\Delta E = 50$ MeV, $\Delta t = 0.1$ ns). The first bunches of the injected batch have a larger phase error (up to 0.3 ns and linearly decreasing) to simulate the effect of the transient beam-loading of the SPS travelling wave structures. Fig. 7b shows the same data after 100 turns. Since the cavities are working as longitudinal damper (gain 2.5 10^{16} V/(s/turn)), the quadrature voltage (in phase with the beam, blue) follows the bunch energy deviation (red bars) and is about zero during the first batch (already attenuated) but larger during the second batch. Fig. 7c shows the situation after 1000 machine turns (about 90 ms) when damping is achieved. We see that the second batch resembles the first one now and we are ready to receive the third one. For completeness, Fig. 7d shows the case of a disabled one-turn feedback after 4400 turns (about 400 ms). The newly injected batch is driven unstable instead of being attenuated[2].

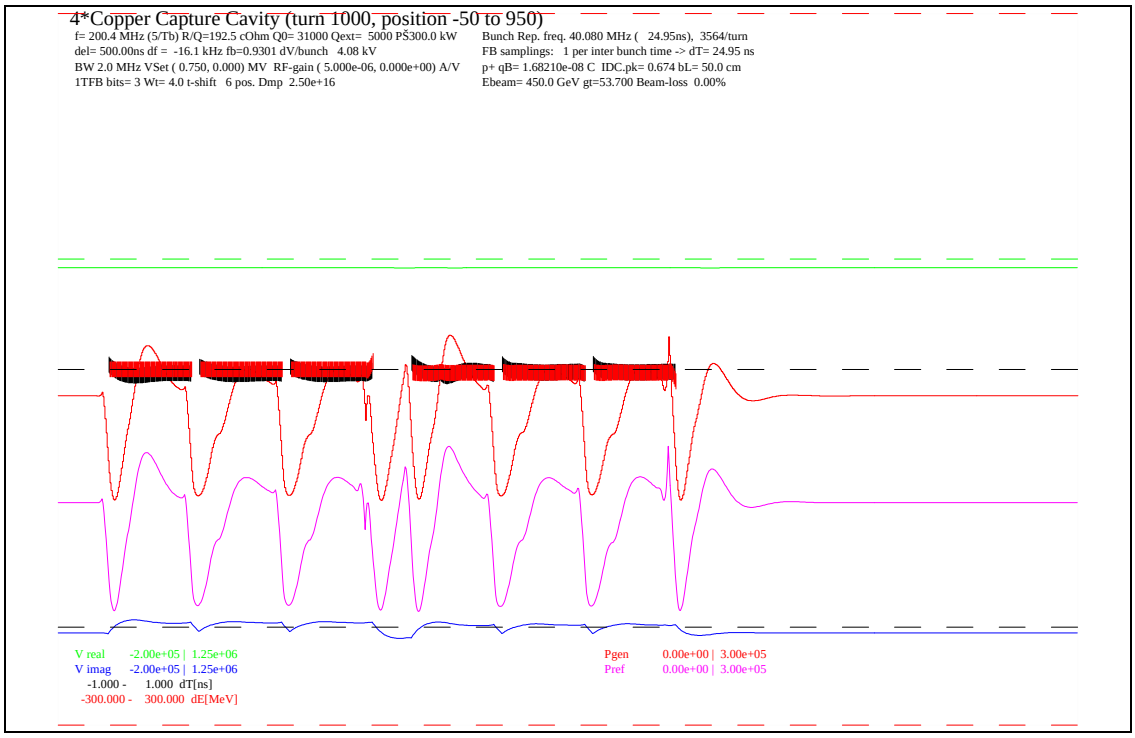

Fig. 7c. After 1000 turns with 1-turn delay feedback. Longitudinal damping has achieved its goal.

The RF reacts in Fig. 7a to 7c slightly before the batches are coming. This is no program error but the one-turn-delay feedback 'knows' in advance what will happen from the last turn. This advance reaction is clearly absent in Fig. 7d where the one-turn-delay feedback was disabled.

Another important fact can be seen in Fig. 7d and especially in 7e,f. During transients the *reflected* power can become considerably higher than the maximum installed RF power.

[2] due to the low gain in this case the voltage set-value had to be 0.85 MV to obtain 0.75 MV

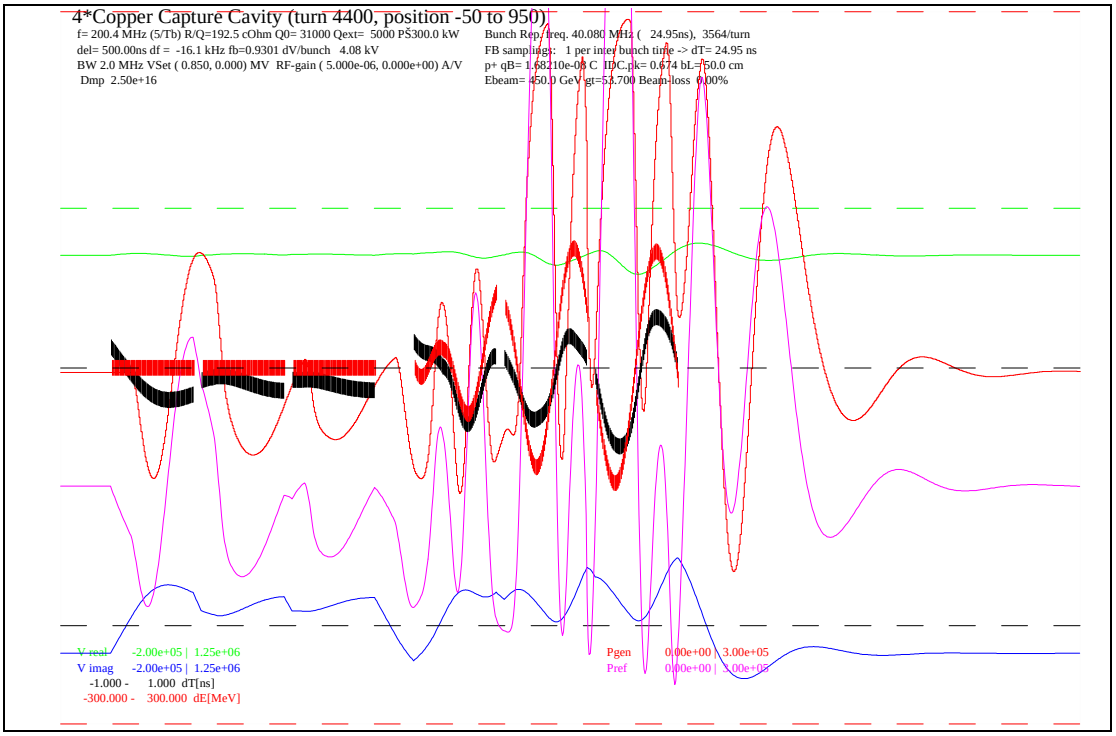

Fig. 7d. Without 1-turn delay feedback. Even after 4400 turns longitudinal damping did not achieve its goal but excited the beam.

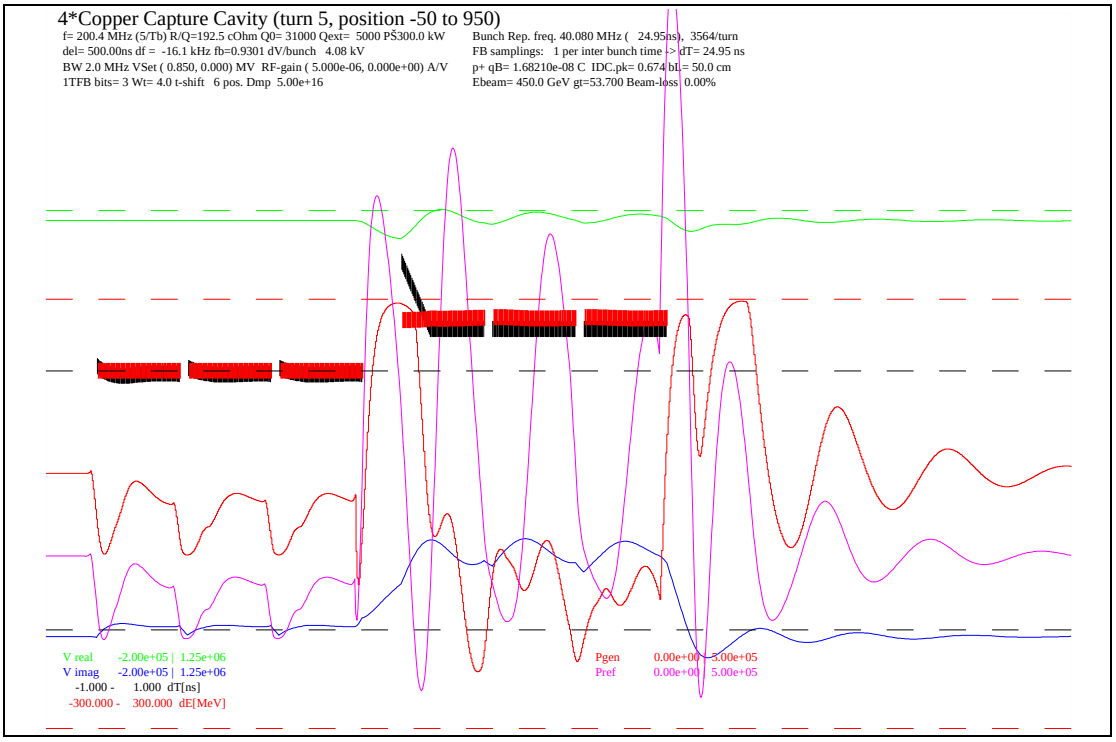

Fig. 7e Twice the damper gain (5 10^{16} V/(s/turn) forces reflected power far above the design limits (power range 0-500 kW, other plots 0-300 kW) Worst case at turn 5

We find e.g. a peak of more than 400 kW for the exceptional case in Fig. 7d (out of range). Here the beam is unstable and deviates from the nominal energy. The damper mode of the cavity counteracts in changing rapidly the generator current, resulting in large reflected power. In reality this beam should have been dumped long before: to protect the equipment against these abnormal cases it is necessary to apply an interlock on the reflected power connected to the beam dump.

.

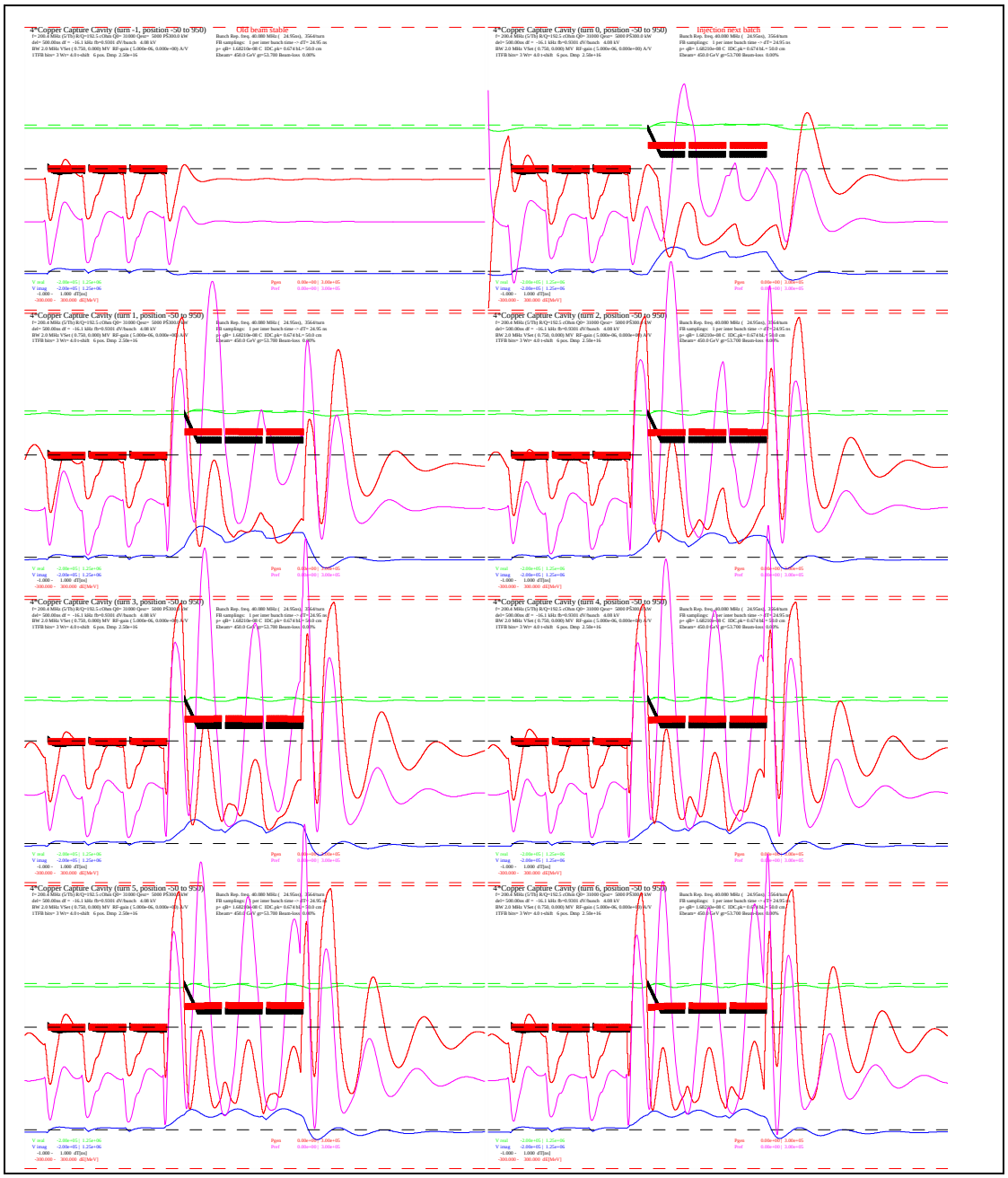

Fig. 7f: First six turns with standard damper gain 2.5 10^{16} V/(s/turn)

Fig. 7e shows another case where a damper gain of 5 10^{16} V/(s/turn) was chosen, *twice* the one for the other plots. This damps very rapidly (800 turns) and gives a stable beam. Therefore we intended to operate the system with this setting. However, e.g. after 5 turns the damper mode tries to empty the cavity by force and a peak reflected power of 500 kW is

observed, much larger than the installed RF power and with a *stable beam* which we would not like to dump. A similar but reduced effect is still present with the standard damper gain ($2.5\ 10^{16}$ V/(s/turn))). A peak of about 400 kW reflected power shows up at turn 5 in Fig. 7f. In any case the power couplers, RF lines, circulators and loads have to be designed to withstand the peaks of reflected power for the design generator peak power to cover the *standard* injection procedure with some margin.

4 Conclusion

It is possible to build a 200 MHz capture system for the LHC, which should lead to a much more realistic injection scenario. With four ACN cavities per beam and four SWC amplifiers per cavity, there is a comfortable safety margin to operate the system. Moreover the ACN cavities can be passively damped when not in use, especially during coast. Much equipment can be re-used from the SPS SWC system (the amplifiers and their power supplies, tuners, damping loops and possibly HOM couplers), making the design of the system simpler and faster, not to mention giving important cost savings. The design of the cavities themselves is in good shape and ready for specification. The RF lines and circulators must be able to withstand large peaks of RF power.

References

[i] J. Tückmantel, The SPS/LHC longitudinal interface, Proc. Workshop on LEP-SPS Performance, Chamonix 1999, pp. 61-68, CERN-SL-99-007 DI.

[ii] The Large Hadron Collider, Conceptual Design, CERN/AC/95-05.

[iii] D. Boussard, D. Brandt, L. Vos, Is a longitudinal feedback system required for LHC?, LHC Project Note 205.

[iv] V. Rödel, Higher order modes and tuning of the SPS 200 MHz single-cell cavity, SL/RFS/Note 91-08.

[v] A. Chao, M. Tigner (editors), Handbook of Accelerator Physics and Engineering, World Scientific, 1999, p. 111.